Published in final edited form as:
Angew Chem Int Ed Engl. 2009 ; 48(50): 9498–9502. doi:10.1002/anie.200902727.

Nanoscale Integration of Sensitizing Chromophores and Porphyrins Using Bacteriophage MS2

Nicholas Stephanopoulos, **Zachary M. Carrico**, and **Prof. Matthew B. Francis**
Department of Chemistry, University of California, Berkeley and Materials Sciences Division, Lawrence Berkeley National Laboratory, Berkeley, CA 94720 USA, Fax: (+1) 510-643-3079

Matthew B. Francis: francis@cchem.berkeley.edu

Keywords

Virus; Energy transfer; Porphyrin; Photocatalysis; Bioconjugation

Photosynthetic systems integrate broad-spectrum light harvesting arrays with reaction centers that generate a charge separation upon photo-excitation.[1,2] To optimize energy and electron transfer, the distances between the individual components are established with nanometer precision by self-assembling scaffolds of multiple membrane-bound proteins.[3] Numerous investigations have sought to mimic this arrangement of chemical moieties for energy conversion applications,[4] commonly using porphyrins as the final electron transfer components. As examples, porphyrins have been arranged into nanometer-scale arrays using covalent linkages,[5–7] hydrogen bonds, and metal coordination.[8,9] In terms of polymeric structures, dendritic architectures have been used with particular success for the construction of porphyrin-based photocatalytic materials.[10–16]

As larger and increasingly complex systems are developed, it becomes difficult to mimic the long-scale rigidity necessary for optimal energy transfer. Although not impossible, it also becomes synthetically cumbersome to install large numbers of porphyrins and other components while maintaining control of positioning and solubility properties. An alternative and potentially highly efficient synthetic strategy is provided by the self-assembling proteins that comprise viral capsids, as their multiple subunits can be modified with chemoselective bioconjugation reactions to position synthetic groups in specified locations. With a view toward making photocatalytic or chemically catalytic materials, porphyrins have been templated noncovalently by the surface of bacteriophage M13 to allow sensitization by tryptophan residues in the coat proteins,[17] iron porphyrins have been captured using poly(His) tags introduced into the cowpea mosaic virus coat protein,[18] and the coat proteins of the tobacco mosaic virus (TMV) have been used to arrange both fluorescent dyes[19] and porphyrins[20] within the virus's RNA binding channel.

An important next step in this field involves attaching several different *types* of groups to the protein scaffolds, a goal that requires multiple site-selective bioconjugation reactions. In this paper we demonstrate this concept by using a multistep synthetic protocol to arrange fluorescent dyes and a zinc porphyrin on the surface of bacteriophage MS2. This positioning allows energy transfer and sensitization of the porphyrin at previously unusable wavelengths, as demonstrated by the system's ability to effect a photocatalytic reduction reaction at multiple excitation wavelengths.

Correspondence to: Matthew B. Francis, francis@cchem.berkeley.edu.

The protein shell of bacteriophage MS2 is comprised of 180 identical monomers arranged in a 27 nm hollow shell. The protein subunits can be expressed recombinantly in *E. coli*, and are obtained as fully assembled monodisperse capsids that are stable from pH 3–10 and temperatures approaching 60 °C.[21–23] Thirty-two 1.8 nm holes allow appreciably large reagents to enter the structures for interior surface modification.[21,24] To access photocatalytic materials, we chose to attach donor chromophores to the interior surface of MS2 and to position zinc porphyrins capable of electron transfer on the exterior, Figure 1a. Such an arrangement would function *via* fluorescence resonance energy transfer (FRET) through the 2 nm protein shell. Zinc porphyrin photocatalysts have been used in a variety of energy conversion schemes[25–27] due to their ability to transfer electrons to carbon nanotubes or fullerenes,[28,29] or to electron carriers like methyl viologen (MV^{2+}) that can be used to produce H_2, NADH, NADPH, and lactic acid.[27,30,31]

We targeted the interior of the capsid by changing the native N87 residue to a cysteine, allowing it to be modified using maleimide-containing dyes, Figure 1b. We chose dyes that absorb at wavelengths where the porphyrin does not, and with emission spectra that overlap a particular porphyrin absorbance band. Alexa Fluor 350 (**1**) was chosen to sensitize the porphyrin Soret band at 424 nm, and Oregon Green 488 (**2**) was selected to target the first porphyrin Q band at 557 nm, Figure 2. Reaction of the capsids with 20 equivalents of the maleimide dyes for 2 hours at room temperature resulted in complete modification of the monomers (corresponding to 180 dyes/capsid), as monitored by ESI-MS (Supporting Information Figure S2). Furthermore, the small Stokes shift of **2** allows for FRET to occur between apposed donor dyes, as the distance between adjacent C87 residues (0.9 to 3.7 nm)[22] is below the Förster radius of 4.0 nm for FRET between two molecules of **2**.[19] The capsid's two native cysteine residues proved unreactive towards the modification conditions (see Supporting Information Figure S7).

There are six lysines on each monomer, so NHS-ester based modification methods[24] would not be suitable for installing a single porphyrin per capsid monomer. Instead, we targeted the artificial amino acid *p*-amino phenylalanine (*p*AF), which we previously showed[32] can be incorporated into MS2 capsids using the Schultz amber codon suppression technique.[33,34] The N87C/T19*p*AF MS2 double mutant was used in all experiments described herein and was obtained by recombinant expression in *E. coli* possessing the appropriate ^{t}RNA and aminoacyl ^{t}RNA synthetase with a yield of 10 mg/L of culture.

Previously we reported the coupling of phenylene diamine derivatives to *p*AF in 30–60 minutes using aqueous periodate.[32,35] We have since found that *N,N*-dimethyl anisidine derivatives couple to this residue with equivalent chemoselectivity in only a few minutes (S.I. Figure S8), allowing the rapid installation of up to 180 copies of aldehyde **3** on the capsid exterior (Figure 1c). We subsequently modified the aldehyde using aminooxy-containing porphyrin **4**, synthesized by adapting known literature protocols,[20,36,37] in concentrations ranging from 20 mM to 2.5 mM. Figure 3c shows the degree of porphyrin attachment relative to the donor dye, determined by comparing the extinction coefficients of the Soret band of **4** with the absorbance maximum of donor **1** or **2**. Capsids without aldehyde **3** showed only minimal noncovalent association of the dyes (see Supporting Information). Although the porphyrins can also be attached to *p*AF in a single step, we chose instead to develop this two-step bioconjugation procedure to allow the future attachment of metal catalysts that would be sensitive to the periodate used in the oxidative coupling reaction. The doubly-modified capsids position the dyes and porphyrins in a range of 2.4 to 3.1 nm from one another, as measured between the residues to which they are attached.[22] The capsids remained intact and water soluble throughout all synthetic steps, as determined by size-exclusion chromatography and transmission electron microscopy (S.I. Figure S3 and S14).

To detect FRET from the dyes inside the capsids to the porphyrins on the outside, we obtained excitation spectra for the conjugates by monitoring the porphyrin fluorescence (Figure 4). The capsids showed porphyrin fluorescence upon excitation of donor **1** or **2**, indicating that energy transfer did indeed occur through the protein shell. Systems with fewer porphyrins per donor resulted in a greater excitation contribution at the donor's wavelength, relative to the porphyrin's excitation band. This indicated that a greater number of dyes contributed to the fluorescence of any single porphyrin.

The energy transfer was further confirmed by monitoring the quenching of the donor emission by the porphyrin. The emission spectra upon excitation at either 350 nm (for **1**) or 500 nm (for **2**) are shown in Figure 5a and 5b. The normalized spectra for capsids containing either donor **1** or donor **2** (as well as aldehyde **3**) but *lacking* acceptor **4** are also shown. The decreasing donor emission, as well as the increasing porphyrin fluorescence emission in Figures 5c and 5d, further demonstrated energy transfer.

We next investigated the porphyrin's electron transfer ability because this property is a more relevant way to use the transferred energy. The excited state of zinc porphyrins can reduce the methyl viologen dication (MV^{2+}) to its radical cation ($MV^{+\cdot}$), which can be monitored by its absorbance at 605 nm.[27,30] By including 2-mercaptoethanol as a sacrificial reductant, the porphyrin cation that is generated can be reduced to close the catalytic cycle (Figure 6a). Because the peak of the solar spectrum lies around 500 nm,[38] we used capsids containing donor **2** for these investigations and illuminated them with 505 nm light from a home-built LED lamp. We evaluated capsids with porphyrin **4** but no donor (system A), with donor **2** but no porphyrin (system B), or with both donor **2** and porphyrin **4** (system C) in a ratio of 3:1. The solutions also contained 150 mM MV^{2+} and 200 mM 2-mercaptoethanol. For systems A and C, the porphyrin concentration was approximately 300 nM, and all quantities of $MV^{+\cdot}$ produced were normalized to that of system C. Upon illumination at 505 nm for 15 minutes, system C showed a significantly higher $MV^{+\cdot}$ production (134 turnovers/porphyrin) compared to system A (38 turnovers/porphyrin) as shown in Figure 6b. This corresponds to a 3.5-fold increase due to the sensitization by donor **2**.

Interestingly, system B (containing donor **2** and aldehyde **3** but no porphyrin) also produced $MV^{+\cdot}$ upon illumination (Figure 6b), but only a quarter of that produced by system C. This indicated that energy transfer to porphyrin **4** in system C plays a vital role in the electron transfer process. Control experiments using free dye **2** (but no MS2 or porphyrin **4**) also produced $MV^{+\cdot}$, confirming that the dye was responsible for the reduction of MV^{2+} and not the capsids, the oxidative coupling linkage, or aldehyde **3**.

We also used a commercially available LED lamp with peak emission at 415 nm to irradiate the Soret band of porphyrin **4** directly. Systems A and C both produced similar amounts of $MV^{+\cdot}$ with or without donor **2** (Figure 6c), confirming that the increased production of $MV^{+\cdot}$ at 505 nm was not a consequence of intrinsic differences in porphyrin activity, but rather that it could be attributed to energy transfer from **2**. All these results indicated that we have indeed sensitized the porphyrin to function catalytically at new wavelengths using our nanoscale integrated system.

In conclusion, we have used the rigid protein scaffold of bacteriophage MS2 to construct an integrated, nanoscale system that positions sensitizing dyes and a photocatalytic porphyrin in specific locations. Our modified capsids allow energy transfer from the inside to the outside of the structures, sensitizing the porphyrin at previously inaccessible wavelengths and allowing broad-spectrum catalytic activity. In principle, our system can be used with any combination of maleimide and aminooxy reagents, allowing considerable flexibility in choosing an appropriate donor for a given acceptor. Current efforts are thus underway to

build similar integrated systems using phthalocyanines[40] and ruthenium bipyridine[41] complexes as the active catalysts. As a general method, the integration of two different chemical groups at precisely defined locations demonstrates the power and flexibility of using viral capsids as nanoscale scaffolds, and will provide a route for both applied and fundamental investigations of complex photocatalytic systems in the future.

Acknowledgments

This work was supported by the Director, Office of Science, Materials Sciences and Engineering Division, of the U.S. Department of Energy under Contract No. DE-AC02-05CH11231. Stipend and tuition support was provided for NS (T32GM008352) and ZC (1 T32 GMO66698) by graduate research training grants from the NIH.

References

1. Nelson N, Ben-Shem A. Nat Rev Mol Cell Biol. 2004; 5:971–982. [PubMed: 15573135]
2. Hu X, Ritz T, Damjanovic A, Autenrieth F, Schulten KQ. Rev Biophys. 2002; 35:1–62.
3. Freer A, Prince S, Sauer K, Papiz M, Lawless AH, McDermott G, Cogdell R, Isaacs NW. Structure. 1996; 4:449–462. [PubMed: 8740367]
4. Gust D, Moore TA, Moore AL. Acc Chem Res. 2001; 34:40–48. [PubMed: 11170355]
5. Wagner RW, Johnson TE, Lindsey JS. J Am Chem Soc. 1996; 118:11166–11180.
6. Prathapan S, Yang SI, Seth J, Miller MA, Bocian DF, Holten D, Lindsey JS. J Phys Chem B. 2001; 105:8237–8248.
7. Holten D, Bocian DF, Lindsey JS. Acc Chem Res. 2002; 35:57–69. [PubMed: 11790089]
8. Drain CM, Varotto A, Radivojevic I. Chem Rev. 2009; 109:1630–1658. [PubMed: 19253946]
9. Beletskaya I, Tyurin VS, Tsivadze AY, Guilard R, Stern C. Chem Rev. 2009; 109:1659–1713. [PubMed: 19301872]
10. Choi M, Aida T, Yamazaki T, Yamazaki I. Angew Chem Int Ed. 2001; 113:3294–3298.
11. Li W, Kim KS, Jiang D, Tanaka H, Kawai T, Kwon JH, Kim D, Aida T. J Am Chem Soc. 2006; 128:10527–10532. [PubMed: 16895420]
12. Yang J, Cho S, Yoo H, Park J, Li W, Aida T, Kim D. J Phys Chem A. 2008; 112:6869–6876. [PubMed: 18610946]
13. Choi M, Aida T, Yamazaki T, Yamazaki I. Chem Eur J. 2002; 8:2667–2678.
14. Hecht S, Ihre H, Frechet JMJ. J Am Chem Soc. 1999; 121:9239–9240.
15. Dichtel WR, Serin JM, Edder C, Frechet JMJ, Matuszewski M, Tan L, Ohulchanskyy TY, Prasad PN. J Am Chem Soc. 2004; 126:5380–5381. [PubMed: 15113208]
16. Dichtel WR, Hecht S, Frechet JMJ. Org Lett. 2005; 7:4451–4454. [PubMed: 16178556]
17. Scolaro LM, Castriciano MA, Romeo A, Micali N, Angelini N, Lo Passo C, Felici F. J Am Chem Soc. 2006; 128:7446–7447. [PubMed: 16756291]
18. Prashun DE Jr, Kuzelka J, Strable E, Udit AK, Cho S, Lander GC, Quispe JD, Diers JR, Bocian DF, Potter C, Carragher B, Finn MG. Chem Biol. 2008; 15:513–519. [PubMed: 18482703]
19. Miller RA, Presley AD, Francis MB. J Am Chem Soc. 2007; 129:3104–3109. [PubMed: 17319656]
20. Endo M, Fujitsuka M, Majima T. Chem Eur J. 2007; 13:8660–8666. [PubMed: 17849494]
21. Hooker JM, Kovacs EW, Francis MB. J Am Chem Soc. 2004; 126:3718–3719. [PubMed: 15038717]
22. Valegard K, Liljas L, Fridborg K, Unge T. Nature. 1990; 345:36–41. [PubMed: 2330049]
23. Mastico RA, Talbot SJ, Stockley PG. J Gen Virol. 1993; 74:541–548. [PubMed: 7682249]
24. Kovacs EW, Hooker JM, Romanini DW, Holder PG, Berry KE, Francis MB. Bioconjugate Chem. 2007; 18:1140–1147.
25. Kadish, KM. The Porphyrin Handbook. 1. Vol. 1–10. Academic Press; 1999.
26. Kadish, K.; Smith, KM.; Guilard, R. The Porphyrin Handbook. 1. Vol. 11–20. Academic Press; 2003.

27. Okura, I. Photosensitization of Porphyrins and Phthalocyanines. 1. Taylor & Francis; 2001.
28. Guldi DM. J Phys Chem B. 2005; 109:11432–11441. [PubMed: 16852399]
29. Guldi DM, Rahman GMA, Zerbetto F, Prato M. Acc Chem Res. 2005; 38:871–878. [PubMed: 16285709]
30. Okura I, Takeuchi M, Kim-Thuan N. Photochem Photobiol. 1981; 33:413–416.
31. Miyatani R, Amao Y. Photochem Photobiol Sci. 2004; 3:681–683. [PubMed: 15239004]
32. Carrico ZM, Romanini DW, Mehl RA, Francis MB. Chem Commun. 2008:1205–1207.
33. Xie J, Schultz PG. Nat Rev Mol Cell Biol. 2006; 7:775–782. [PubMed: 16926858]
34. Mehl RA, Anderson JC, Santoro SW, Wang L, Martin AB, King DS, Horn DM, Schultz PG. J Am Chem Soc. 2003; 125:935–939. [PubMed: 12537491]
35. Hooker JM, Esser-Kahn AP, Francis MB. J Am Chem Soc. 2006; 128:15558–15559. [PubMed: 17147343]
36. Kruper WJ, Chamberlin TA, Kochanny MJ. Org Chem. 1989; 54:2753–2756.
37. Chen Y, Parr T, Holmes AE, Nakanishi K. Bioconjugate Chem. 2008; 19:5–9.
38. ASTM G173-03.: Extraterrestrial Spectrum, Terrestrial Global 37 deg South Facing Tilt & Direct Normal + Circumsolar. ASTM International;
39. http://www.invitrogen.com/site/us/en/home/brands/Molecular-Probes.html
40. Torre GDL, Claessens CG, Torres T. Chem Commun. 2007:2000–2015.
41. Grätzel M. J Photochem Photobio A. 2004; 164:3–14.

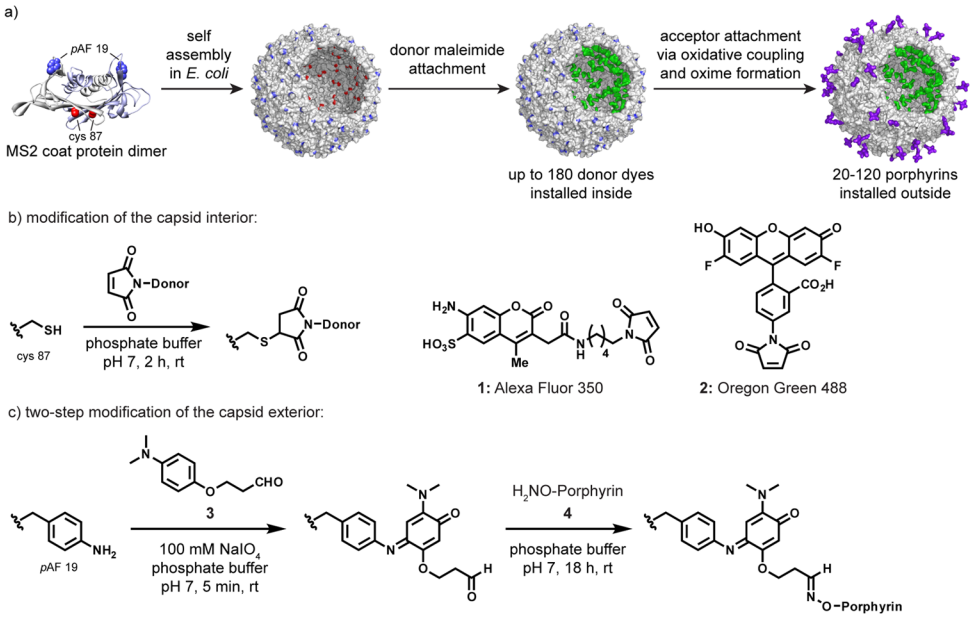

Figure 1.

Modification of N87C T19*p*AF MS2. **a)** Two mutations (N87C and T19*p*AF) were introduced into MS2 coat protein subunits. After capsid formation in *E. coli*, the interior and exterior surfaces were differentially modified using a multistep sequence. **b)** The interior of the capsid was modified at C87 (red) using either AlexaFluor 350 (**1**) or Oregon Green 488 (**2**) maleimide dyes. Up to 180 copies of each chromophore were installed. **c)** The exterior of the capsid was modified first via an oxidative coupling reaction to attach aldehyde **3** to the **p**AF19 groups (blue), and subsequently with aminooxy-containing porphyrin **4** to form stable oxime linkages. This design allows for energy transfer from the dye inside the capsid to the porphyrin on the outside via FRET.

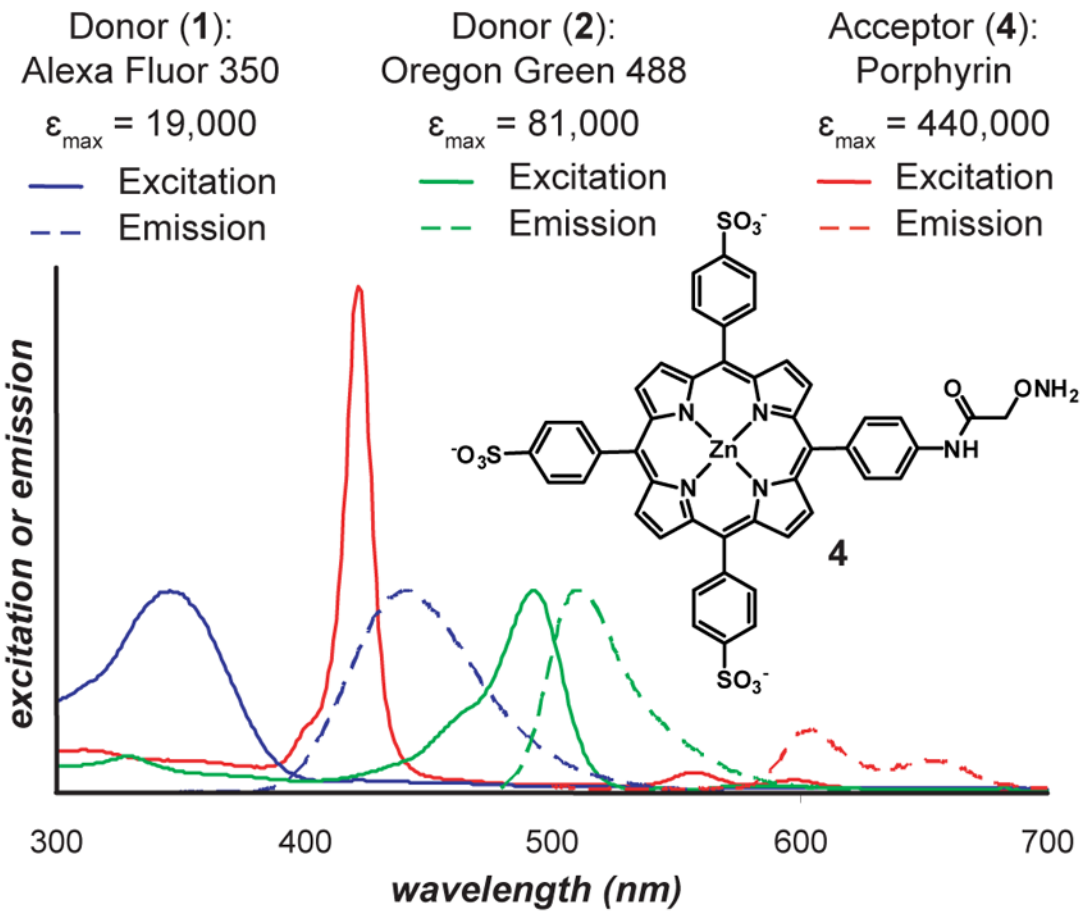

Figure 2.
Comparison of the excitation and emission spectra for the chromophores used in this study. The Alexa Fluor 350 emission overlaps with the porphyrin Soret band, while the Oregon Green 488 emission overlaps with the first porphyrin Q band, allowing for FRET.

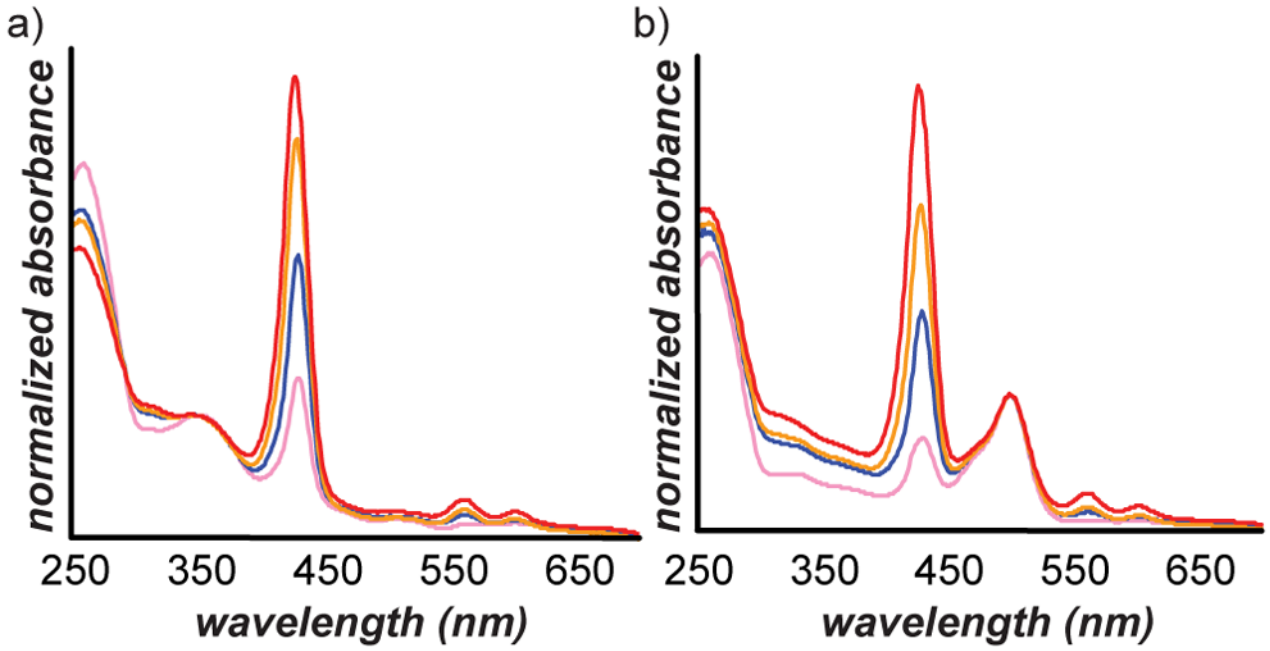

c

Color	[4]	Alexa Fluor 350 (**1**) (**1**):(**4**)	Alexa Fluor 350 (**1**) (**4**)/capsid	Oregon Green (**2**) (**2**):(**4**)	Oregon Green (**2**) (**4**)/capsid
	20 mM	8.5	21	8	23
	100 mM	4.5	40	3.3	55
	500 mM	3	60	2	90
	2.5 mM	2.5	72	1.6	113

Figure 3.

UV-vis spectra of the MS2-AF-porphyrin **(a)** and MS2-OG-porphyrin **(b)** systems. The spectra are normalized at the absorbance maximum of the donor dye. **c)** The ratio of donors to porphyrins was calculated by comparing the absorbance ratios and using the extinction coefficients listed in Figure 2. The number of porphyrins per capsid was calculated by assuming complete dye conversion and dividing the total number of monomers (180) by the number of dyes per porphyrin.

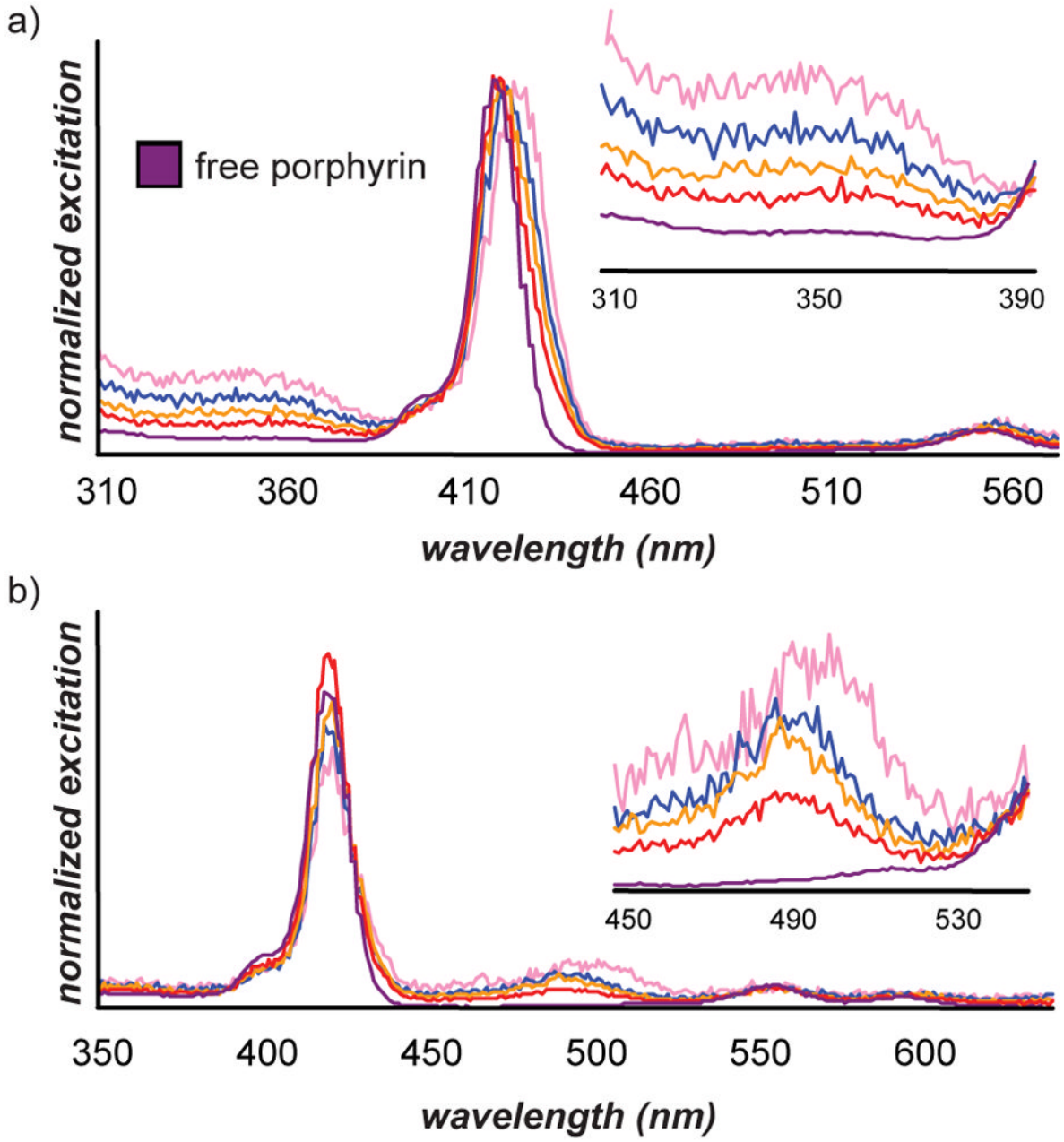

Figure 4.

Excitation spectra of the MS2-1-4 **(a)** and MS2-2-4 **(b)** conjugates. The insets show expansions of the areas of maximum donor excitation. The MS2-**1**-**4** spectra were normalized at the porphyrin Soret band and excitation was monitored at the first porphyrin emission band at 602 nm. The MS2-**2**-**4** spectra were normalized at the first porphyrin Q band and excitation was monitored at the second porphyrin emission band at 655 nm to minimize any residual fluorescence emission from the Oregon Green. The colors correspond to the chromophore ratios listed in Figure 3c. The slight red-shift seen at lower modification levels is possibly due to coordination of the two surface-accessible exterior lysines to the zinc center.

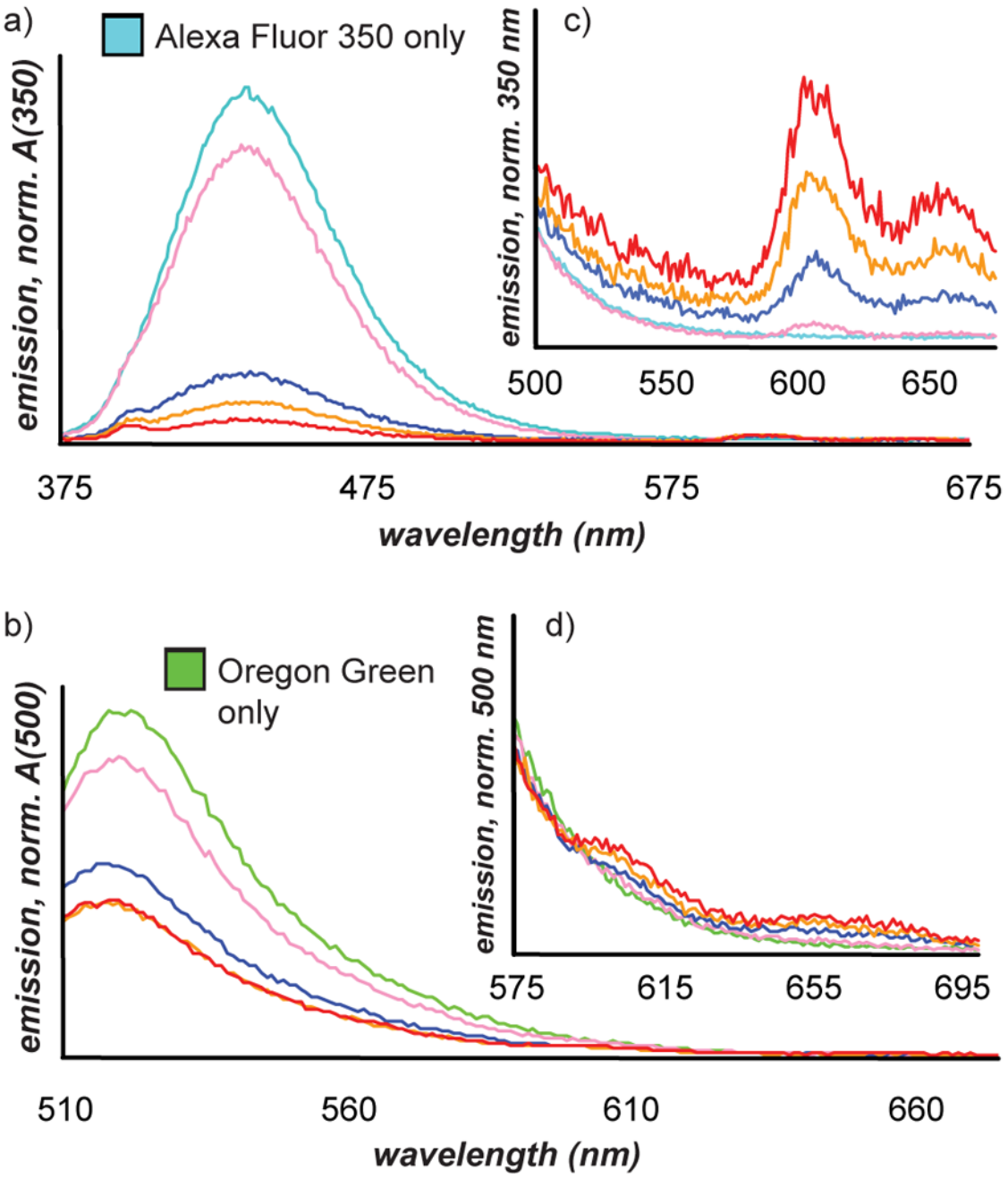

Figure 5.

Emission spectra upon donor excitation for the MS2-**1**-**4 (a)** and the MS2-**2**-**4 (b)** systems, with emission normalized by the donor absorbance. Increased amounts of porphyrin result in greater dye quenching due to energy transfer. The insets show the emission of the porphyrin in the MS2-**1**-**4 (c)** and MS2-**2**-**4 (d)** systems, normalized at the donor emission maximum to demonstrate the relationship between donor quenching and acceptor emission. The two porphyrin emission bands at 602 and 655 nm are clearly visible.

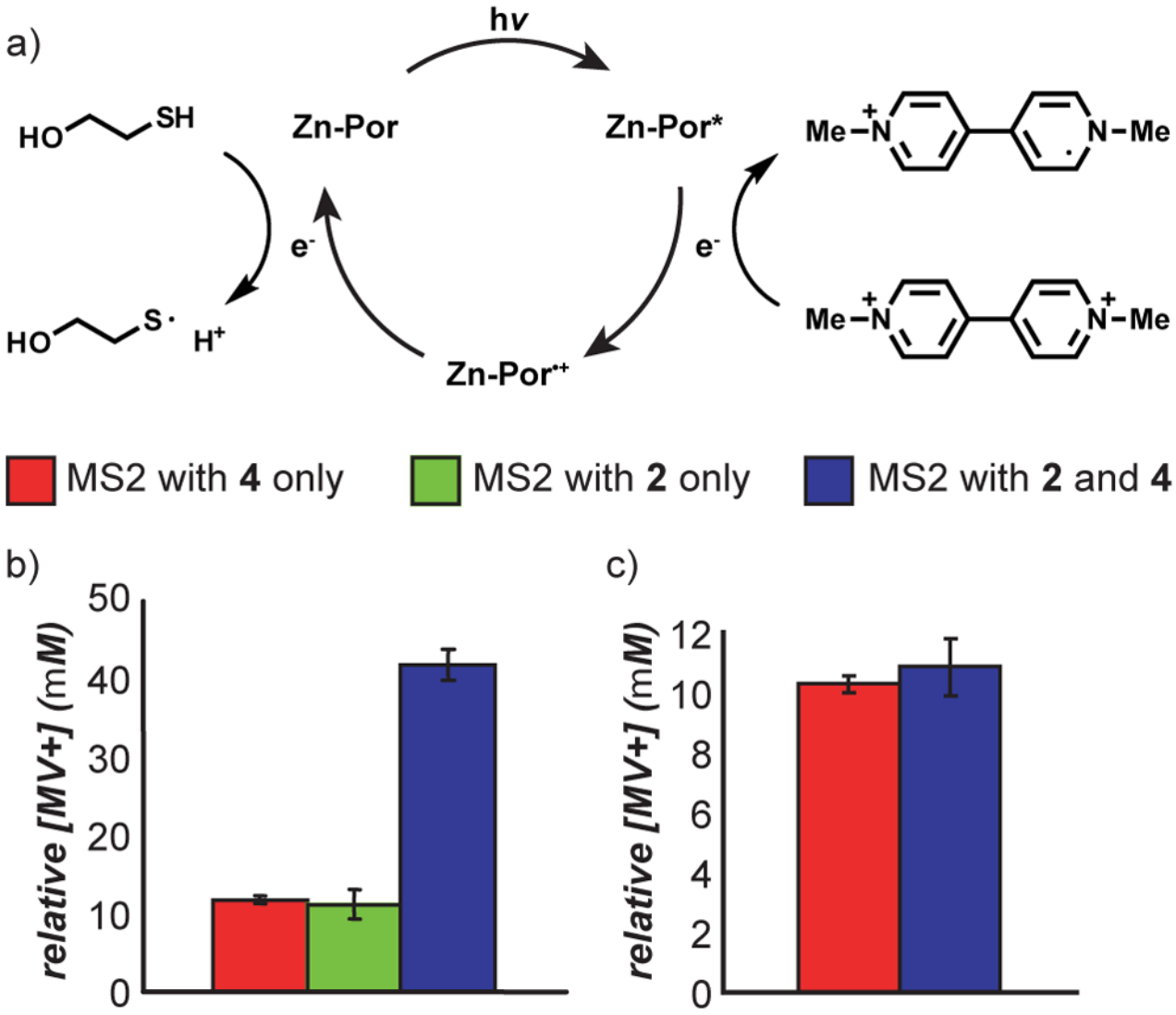

Figure 6.

Photoreduction of methyl viologen **(a)** by a sensitized porphyrin system with 15 min illumination at 505 nm **(b)** and 0.5 min illumination at 415 nm **(c)**. The different time values were required due to the extinction coefficient differences between 2 and 4. Values represent the average and standard deviations of n = 3 measurements.